Water Resources Research

RESEARCH ARTICLE
10.1029/2019WR025251

Special Section:
Advances in remote sensing, measurement, and simulation of seasonal snow

Quantifying Uncertainties in Snow Depth Mapping From Structure From Motion Photogrammetry in an Alpine Area

Jason Goetz[1] and Alexander Brenning[1]

[1]Department of Geography, Friedrich-Schiller-University Jena, Jena, Germany

Abstract Mapping snow conditions in alpine areas is crucial for monitoring local hydrology to support water resource management decisions. Recently, the use of structure-from-motion multiview stereo 3-D reconstruction (or SFM photogrammetry) to derive high-resolution digital elevation models (DEMs) has become popular for mapping snow depth in alpine areas. In this study, methods for communicating spatial uncertainties in snow depth calculated from SFM-derived DEMs are presented using a case study in the French Alps. A spatially varying snow depth precision estimate was determined using an error propagation model based on the precision of the acquired SFM DEMs, which was obtained from repeated unmanned aerial vehicle flights. Spatially varying snow depth detection limits were determined using Student's *t* distribution. It was found that snow depths as shallow as 1 to 5 cm could be detected with high confidence for most of the study area. Areas of high uncertainties were generally related to where the extent of the ground control coverage did not match in the snow-on and snow-off surveys and in areas with higher surface roughness. A map of the snow depth detection threshold was found to be useful for identifying areas with high uncertainties and potential biases in the SFM snow depths, such as errors due to changes in topography between DEM acquisition dates and poor SFM reconstruction.

Key Points:
- Spatially varying structure-from-motion precision estimates can be used to communicate snow depth measurement uncertainties
- Structure-from-motion derived snow depths from unmanned-aerial-vehicle imagery can detect shallow depths (1–5 cm) with high confidence
- Repeated UAV surveys can be used as a robust approach for estimating SFM DEM precision for various snow-covered terrain conditions

Correspondence to:
J. Goetz,
jason.goetz@uni-jena.de

Citation:
Goetz, J., & Brenning, A. (2019). Quantifying uncertainties in snow depth mapping from structure from motion photogrammetry in an alpine area. *Water Resources Research*, *55*, 7772–7783. https://doi.org/10.1029/2019WR025251

Received 28 MAR 2019
Accepted 23 AUG 2019
Accepted article online 30 AUG 2019
Published online 9 SEP 2019

1. Introduction

Snow is an important water resource in many mountain regions around the world. Given the changing climate can reduce the water availability in these snow-dominated regions (Barnett et al., 2005; Lemke et al., 2007; Middelkoop et al., 2001), accurate monitoring and forecasting of seasonal changes in snow distribution remain crucial for effective water resources management. Accurate knowledge of snow accumulation can also help us improve our understanding of environmental processes in mountain areas including changes in ground temperatures (Apaloo et al., 2012; Luetschg & Haeberli, 2007), permafrost creep (Delaloye et al., 2010; Ikeda et al., 2008), avalanches (Bühler et al., 2011), rockfalls (Haberkorn et al., 2016), landslides (Matsuura et al., 2003; Okamoto et al., 2018), glacier dynamics (Immerzeel et al., 2014; Rossini et al., 2018), and vegetation growth (Jonas et al., 2008). Additionally, high-resolution snow pack data can be used as reference data to test the accuracy of satellite remote-sensing products (Marti et al., 2016; Tinkham et al., 2014).

Structure-from-motion multiview stereo 3-D reconstruction (also known as SFM photogrammetry) is a rapidly emerging technique for high-resolution snow depth mapping in alpine environments. In general, SFM can create a 3-D reconstruction of a surface using a collection of images taken from different viewing angles (Snavely et al., 2006). Typically, these images are acquired using unmanned aerial vehicles (UAVs; Adams et al., 2018). When SFM techniques are applied for topographic analysis, they can be used to produce high-resolution digital elevation models (DEMs) of Earth's surface (Fonstad et al., 2013; James & Robson, 2012; Westoby et al., 2012). Like lidar and digital photogrammetry methods, SFM-derived snow depth maps are computed by differencing two coregistered elevation models acquired for snow-covered (snow-on) and snow-free (snow-off) conditions. Reported snow depth root mean squared errors (RMSEs) using UAVs in alpine areas typically range between 7 and 30 cm (Adams et al., 2018; Avanzi et al., 2018; Bühler et al., 2016; de Michele et al., 2016; Harder et al., 2016; Vander Jagt et al., 2015).

Although SFM-derived snow depth maps have shown promise to obtain frequent observations of snow distribution with a high spatial resolution, as with the other techniques, there are challenges to produce reliable and accurate data. These challenges are related to uncertainties inherent in elevation differencing, which are

controlled by the elevation models' quality (Wechsler & Kroll, 2006; Wheaton et al., 2010) and coregistration accuracy (Bernard et al., 2017; James et al., 2017; Marti et al., 2016; Nuth & Kääb, 2011). Understanding and quantifying the uncertainties in elevation model differencing can help us differentiate the computed surface change observations from noise (Wheaton et al., 2010). Or in the case of mapping snow distribution, it can help us determine detection limits of the computed snow depth. Calculating the propagation of elevation model errors is typically used for estimating the uncertainty when analyzing surface changes (Brasington et al., 2000; James, Robson, Smith, et al., 2017; Lane et al., 2003; Wheaton et al., 2010). Uncertainties in SFM-derived elevation models are usually assessed by a comparison with a spatially distributed set of reference data, typically acquired using lidar, differential/kinematic Global Navigation Satellite System (GNSS), or total-station survey data (Goetz et al., 2018; James & Robson, 2012; Smith et al., 2015; Westoby et al., 2012).

The quality of the SFM-derived elevation models for snow depth mapping generally depends on field site conditions, survey design, and the SFM software. These aspects can include the snowpack conditions (e.g., the presence of fresh snow or ice; Gindraux et al., 2017; Fernandes et al., 2018; Bühler et al., 2016; Cimoli et al., 2017; Vander Jagt et al., 2015; de Michele et al., 2016), terrain conditions (e.g., hilly or flat; Cimoli et al., 2017; Avanzi et al., 2018), lighting conditions (i.e., presence of shadows; e.g., zenith angle of the sun and cloud coverage; Goetz et al., 2018; Nolan et al., 2015; Cimoli et al., 2017; Harder et al., 2016; Bühler, Adams, Stoffel, et al., 2016; Gindraux et al., 2017), characteristics of the UAV survey (e.g., flying height, image overlap, and distribution of ground control; Goetz et al., 2018; James et al., 2017; Tonkin et al., 2014; Gindraux et al., 2017), and the SFM software processing (e.g., settings for sparse and dense point cloud quality; Cimoli et al., 2017; Hendrickx et al., 2019; Gindraux et al., 2017).

An additional challenge unique to mapping snow depth using elevation differencing is accounting for changes in the surface topography beneath the snow cover that may occur overtime. For example, seasonal erosion of the surface (Avanzi et al., 2018; Bernard et al., 2017), frost heave (Nolan et al., 2015), vegetation compression (Nolan et al., 2015), and permafrost creep (Goetz et al., 2019) can cause errors in the computed snow depths. In the case of monitoring snow accumulation on glaciers, glacier surface lowering due to ice or snow melt and ice flow can also lead to errors (Gindraux et al., 2017).

The purpose of this paper is to spatially characterize uncertainties in snow depths computed from SFM-derived elevation models in an alpine area. Recent work by Adams et al. (2018) and Goetz et al. (2018) have provided initial evidence of how spatially varying SFM precision in the snow-on DEM can contribute to spatially varying uncertainties in SFM snow depths. However, these studies, which use repeated UAV surveys, only explored the spatial variation in uncertainties corresponding to snow-on DEMs. In contrast, our study explores and discusses how both the uncertainties in the snow-on and snow-off DEMs contribute to the spatial distribution of uncertainties in SFM snow depths using an error propagation model. We utilize repeated UAV surveys and in-situ field survey data taken during both snow-on and snow-off elevation model acquisition dates to spatially determine the precision of the derived snow depths. Additionally, we illustrate how spatially varying snow depth detection limits computed using Student's t distribution can help provide insights to potential biases in the SFM snow depths due to a poor SFM model and changes in the topography occurring between the DEM acquisition dates.

2. Materials and Methods

2.1. Study Site and Data Collection

This study was conducted in the Combe de Laurichard (45.01°N, 6.37°E, 2,500 m above sea level), which is located in the French Alps near the Col du Lautaret. The snow depth in the area of an active rock glacier was mapped, the Laurichard rock glacier, to test SFM methods in complex mountain topography. The rock glacier surface is generally composed of large angular boulders and debris formed from densely fractured granite (Bodin et al., 2009). The survey area (~240 m × 210 m) contains the front of a tongue-shaped rock glacier showing compression features such as transverse ridges and furrows. Throughout this paper, the rock glacier area is referred to as active terrain. The stable terrain, which is adjacent to the rock glacier front, has a hummocky topography that contains dense and sparse clusters of large boulders and debris, as well as low vegetation cover.

Aerial imagery acquired from UAV flights for SFM processing and ground-based measurements were collected on 1 June and 5 October 2017. The June date corresponds to the snow-on conditions during the melt period, and 5 October was the snow-off date required for computing snow depth (Figure 1). During the survey on 1 June, the study area was partially snow covered. The snow had a strong texture due to formation of suncups and runnels. The UAV flights were flown in cloud-free conditions with air temperature ranging from 2 to 10 °C. On 5 October, the study area was entirely snow-free. The flights were flown in mainly cloud-free to partially cloud-covered conditions, and the air temperature ranged from 7 to 16 °C.

Repeated UAV surveys were performed on each date to obtain multiple DEMs representing the surface heights. These surveys were conducted using a DJI Phantom 4 quadcopter that was programmed to fly autonomous missions with the Map Pilot app for iOS devices. Each survey was programmed to fly in parallel flight paths with a maximum speed of 7.1 m/s and to fly above the terrain at 60 m above ground level. A Shuttle Radar Topography Mission 1 Arc-Second Global DEM was used for terrain following. The optical imagery (RGB) was acquired at nadir position with a 75% side and front overlap. A shutter-priority mode with a set aperture of f/2.8 and ISO of 100 was used to take the images, which were saved in JPEG format. Artificial targets spread across the study area were used as ground control points (GCPs).

Reference data and the position of the GCPs were surveyed using Real-Time-Kinematic (RTK) GNSS measurements. The errors in the SFM-derived snow-on and snow-off DEMs were determined from surveyed checkpoints of surface heights, which depending on the date, include the height of snow-covered and/or snow-free surfaces. During the snow-on date, manual snow-probe measurements were taken at each checkpoint location using an avalanche snow probe with a maximum depth of 3 m. These probed snow depths were used to measure errors in the SFM-derived snow depths.

Due to the changing topography of the snow-covered surface, the location of the GNSS base station was different during survey dates. To improve the quality of the RTK GNSS measurements, the data were post-processed using GNSS data from the PUYA reference station, which is located approximately 19 km from the study area. The positional accuracies of the RTK GNSS surveys were $\leq$2 cm at 1σ. The spatial reference of this study was based on the RGF93/Lambert-93 projection and the NGF-IGN69 vertical datum (EPSG::5698).

2.2. DEM Processing and Computing Snow Depths

The UAV imagery for each flight was processed using Agisoft's Photoscan (Version 1.4.2) for deriving SFM DEMs. The photos were aligned using a high accuracy with a key point limit of 40,000, a tie point limit of 4,000, and the option for adaptive camera model fitting selected. All intrinsic and extrinsic parameters were optimized. Before optimization, the sparse point cloud was filtered by removing points that had a reprojection error >0.5, a projection accuracy >3.0, and reconstruction uncertainly level >10. Georeferencing and optimization of camera parameters were based on the surveyed GCPs. The dense points matching quality parameter was set to mild. The dense point clouds were exported as DEMs to the software-suggested spatial resolution (<5 cm). All DEMs were resampled to the same 5 cm × 5 cm spatial resolution grid format using bilinear interpolation. The elevation surface for each surveyed date was represented by a mean DEM, which was determined by calculating the mean elevation, $\bar{y}$, for each grid cell from the corresponding repeat DEMs. Snow depths were computed by subtracting the mean elevations, $\bar{y}_{on} - \bar{y}_{off}$, of the mean snow-on and snow-off DEMs. The coregistration of the DEMs relied solely on the accuracy of the georefencing based on the RTK-GNSS-surveyed GCPs. There were no shared GCP targets between the snow-on and snow-off DEMs. This condition was tested to determine what snow depth accuracies may be achievable when snow-free areas are not available for coregistration, which can be the case in this study area during peak accumulation or after recent snowfall.

2.3. Mapping Snow Depth Uncertainties

A spatially varying uncertainty, σ_d, or precision in the SFM snow depths can be expressed by estimating the standard deviation of the propagated error for each grid cell

$$\sigma_d = \sqrt{\sigma_{on}^2 + \sigma_{off}^2}, \quad (1)$$

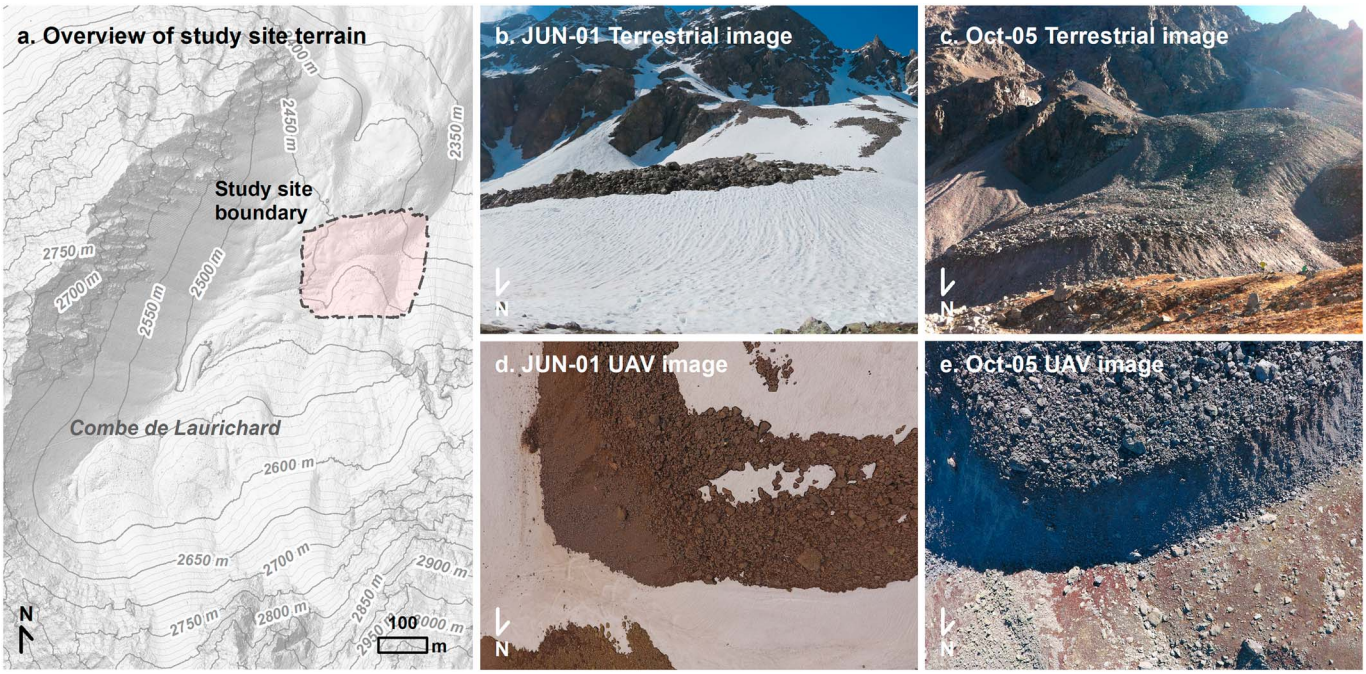

Figure 1. A terrain map illustrating an overview of the study site and unmanned aerial vehicle (UAV) surveyed area (a). Ground-based (b,c) and UAV (d,e) images of the rock glacier taken on the survey dates in 2017.

where σ_{on} and σ_{off} are measures of uncertainty for the snow-on and snow-off DEMs, whose errors are assumed to be independent. Calculating the propagated error standard deviation for DEM differencing is often applied to estimate the uncertainties in topographic change detection (Brasington et al., 2000; James, Robson, Smith, et al., 2017; Lane et al., 2003; Wheaton et al., 2010). Similar to Goetz et al. (2018), the uncertainty or precision in the DEMs was estimated by calculating the standard deviation σ in elevation for each grid cell from the repeatedly acquired SFM DEMs (Table 1). The RMSE was used to determine the accuracy of the DEMs and the snow depths from the GNSS-surveyed validation data. The errors in the DEMs were also characterized by terrain cover: snow cover, fine debris, or rocky debris. The snow depth errors where estimated for stable terrain and active terrain (i.e., on the active rock glacier).

In addition to mapping the precision of the SFM snow depths, the uncertainty in differencing DEMs can be expressed using the minimum level of detection for a given confidence level based on estimates of DEM precision (Brasington et al., 2003; Lane et al., 2003; Wheaton et al., 2010). Since in this study there are repeat observations of the snow-on and snow-off DEMs, the detection limit was expressed as the margin of error corresponding to a one-sided confidence interval using a critical t value. That is, for determining a minimum level of snow depth detection, we are mainly concerned if the SFM snow depths are greater than 0, in this case at a 95% confidence level. In earth sciences (Borradaile, 2002), including topographic change detection studies (Brasington et al., 2003; James, Robson, Smith, et al., 2017; Lague et al., 2013; Wheaton et al., 2010), a 95% confidence level is usually applied. The minimum detected snow depth was determined by

$$\mathrm{LoD}_{95\%\mathrm{CL}} = t^{*}_{\mathrm{df}} \times \sqrt{\frac{\sigma^2_{\mathrm{on}}}{n_{\mathrm{on}}} + \frac{\sigma^2_{\mathrm{off}}}{n_{\mathrm{off}}}}, \tag{2}$$

where σ_{on} and σ_{off} are estimates of the standard deviations of the snow-on and snow-off elevations based on repeat DEM observations, n_{on} and n_{off} are the corresponding numbers of DEMs used for finding $\bar{y}$ and σ, and t^{*}_{df} is the (one-sided) critical t value for the given degrees of freedom, df. These are calculated for each grid cell as

Table 1
Summary of Unmanned Aerial Vehicle Flights Used to Derive Structure-From-Motion Multiview Stereo 3-D Reconstruction Digital Elevation Models for Computing Snow Depth

Date	No. of flights	No. images/flight	No. GCPs	Avg. flying height (m)	Coverage area (km^2)	RMS reproj. error (pixels)	Vertical error from GCPs (cm)
1 Jun	6	67–77	19	59–62	0.056–0.061	0.48–0.70	1.8–2.5
5 Oct	7	92–121	13	62–67	0.078–0.090	0.44–0.51	1.9–3.9

Note. GCP = ground control point; RMS = root mean squared.

$$\mathrm{df} = \left(\frac{\sigma^2_{\mathrm{on}}}{n_{\mathrm{on}}} + \frac{\sigma^2_{\mathrm{off}}}{n_{\mathrm{off}}}\right)^2 \Big/ \left(\frac{1}{n_{\mathrm{on}}-1}\left(\frac{\sigma^2_{\mathrm{on}}}{n_{\mathrm{on}}}\right)^2 + \frac{1}{n_{\mathrm{off}-1}}\left(\frac{\sigma^2_{\mathrm{off}}}{n_{\mathrm{off}}}\right)^2\right). \quad (3)$$

The free-software environment R (Version 3.4.3) was used to perform the statistical analysis and geocomputations in this study. Grid cell calculations were performed using the "raster" package (Version 2.5-8; Hijmans, 2016).

3. Results

3.1. DEM Accuracy and Precision

The smoother snow-covered DEM surface heights had a higher accuracy than the snow-free areas (Table 2), which was predominantly made up of exposed rock debris. Also, the DEM measured surface heights were more accurate for the smoother fine rock debris areas than the rougher rock-debris surfaces such as found on the rock glacier. The overall accuracy, measured by the RMSE, of the DEMs ranged from 7 to 9 cm.

The distribution of DEM errors for the snow-off DEM was generally spatially heterogeneous (Figure 2b). That is, there was no clear sign of a strong systematic error in the elevation surface where the GNSS validation data were sampled. However, there was a cluster of overestimated elevations in the northwest area of the snow-on DEM (Figure 2a). This elevation measurement bias was occurring outside of an area enclosed by the GCPs and where the precision was relatively good (<2 cm; Figure 2d).

The precision of the DEMs was lower where the terrain surface was rougher (i.e., rocky debris cover), further away from ground control, and at the smoothly textured snowdrift located in the southwest area of the snow-on DEM (Figure 2d). The precision throughout the DEMs was mainly less 2 cm. The distribution of precision values was spatially more heterogeneous in the snow-off DEM than the snow-on DEM.

3.2. SFM Snow Depth Uncertainty

The overall RMSE of the snow depths was 15 cm (Table 3). The stable terrain had a higher accuracy (RMSE = 12.2 cm) than the active terrain (18.2 cm). Based on the snow-probe measurements, the snow depths were on average underestimated. However, this may be a result of a measurement bias related to snow probing—the suncups made it difficult to determine the height of the snow to the nearest centimeters. Snow depths that were also computed in the snow-free areas located in the northeast part of the scene show an increasing trend in depth toward the boundary of the study area. This trend may be an indication of where an overestimation in snow depth occurred due to a bias in the snow-on DEM, which was identified with the GNSS measurements. The precision of the SFM snow depths was less than $\sigma = 4$ cm for most of the study area (Figure 2f).

Table 2
Accuracy of DEMs Calculated From Global Navigation Satellite System Surveyed Checkpoints

Mean DEM	No. obs.	RMSE (cm)	Mean (cm)
June (overall)	177	8.7	2.1
Snow cover	106	6.5	0.3
Rocky debris cover	71	11.3	4.8
October (overall)	141	7.4	1.5
Fine debris cover	38	3.8	2.0
Rocky debris cover	103	8.4	1.3

Note. June represents the snow-on DEM, and October the snow-off DEM. DEM = digital elevation model; RMSE = root mean squared error.

At a 95% confidence level, most of the study area had a detection limit between 1 and 5 cm—the median detection limit was 3 cm (Figures 3 and 4). The minimum detectable snow depth ranged from 0.2 to 194 cm. The snow depths in most of the study area were significantly detected. A comparison of the mapped snow-free areas to the areas that were lower than the snow depth detection limit shows possible uncertainties in the computed snow depths (Figure 3). For example, areas that should be below the detection limit because they are snow-free were not

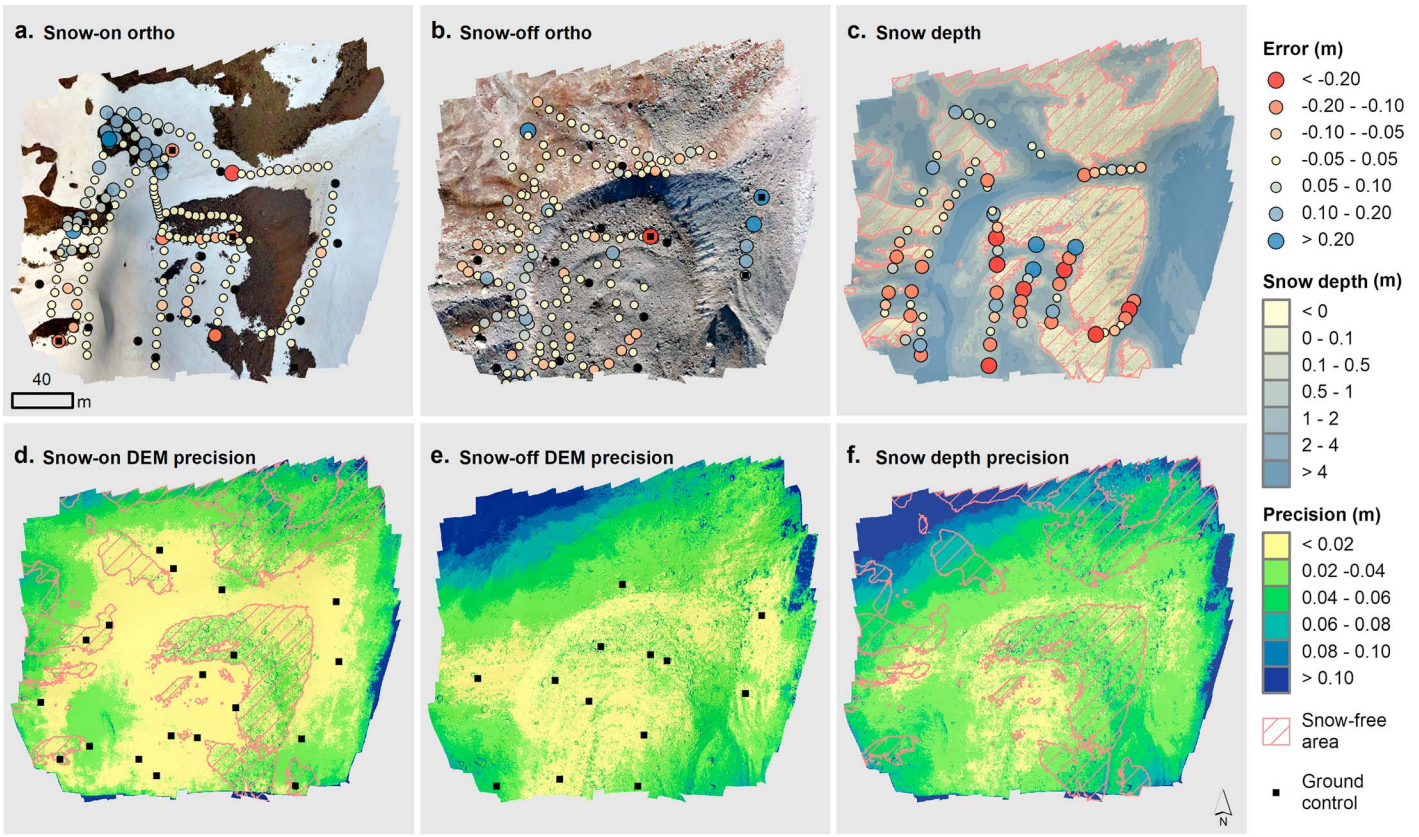

Figure 2. Bubble plots of Global Navigation Satellite System measured digital elevation model (DEM) errors and orthomosaics obtained from unmanned aerial vehicle imagery (a,b). Maps of DEM precision calculated from repeat DEM observations (d,e). Structure-from-motion multiview stereo 3-D reconstruction snow depth map and bubble plot of snow depth accuracies based on snow-probed observations (c) and a structure-from-motion multiview stereo 3-D reconstruction snow depth precision map (f).

(Figure 3e). This is the same area that was overestimated in the snow-on DEM (Figure 2a) and may indicate that there was also a bias in the estimated snow depths surrounding this area. On the active rock glacier, there was a mismatch between the mapped snow-free areas and the ones detected by the threshold limit (Figure 3cd), which can be an indication of a change in the bare-ground topography between the snow-on and snow-off DEM acquisition dates.

4. Discussion

4.1. Mapping Snow Depth Uncertainties

Based on a spatially varying snow depth detection limit, it was shown that SFM snow depths using UAV imagery can detect depths as shallow as 1 cm (Figure 4a). Using snow-probed calculated depth errors, Harder et al. (2016) proposed a global SFM snow detection limit of 30 cm (at 4σ), which would be approximately 15 cm at a 95% confidence level (2σ). For deep snow packs where it is clear that most of the snow depths will exceed the precision, a global limit of snow depth detection may be suitable (Passalacqua et al., 2015). However, a spatially varying snow depth detection limit may be useful for analysis of shallow snow pack since the precision of snow depths, as observed in this study and by Adams et al. (2018), can substantially vary spatially. Spatially varying measures of precision can be used to avoid overly conservative detection limits caused by global thresholds (Lane et al., 2003; Passalacqua et al., 2015; Wheaton et al., 2010).

Table 3
Structure-From-Motion Multiview Stereo 3-D Reconstruction Snow Depth Accuracy Based on Snow-Probed Observations Calculated for the Entire Area (Overall), Active Terrain (i.e., on the Rock Glacier), and Stable Terrain

Terrain	No. obs.	RMSE (cm)	Mean (cm)	Std. dev. (cm)	Median (cm)	IQR (cm)
Overall	80	15.2	−3.6	14.8	−2.4	17.3
Stable	44	12.2	−1.0	12.3	−1.9	12.3
Active	36	18.2	−6.7	17.2	−10.3	26.2

Note. RMSE = root mean squared error; IQR = interquartile range.

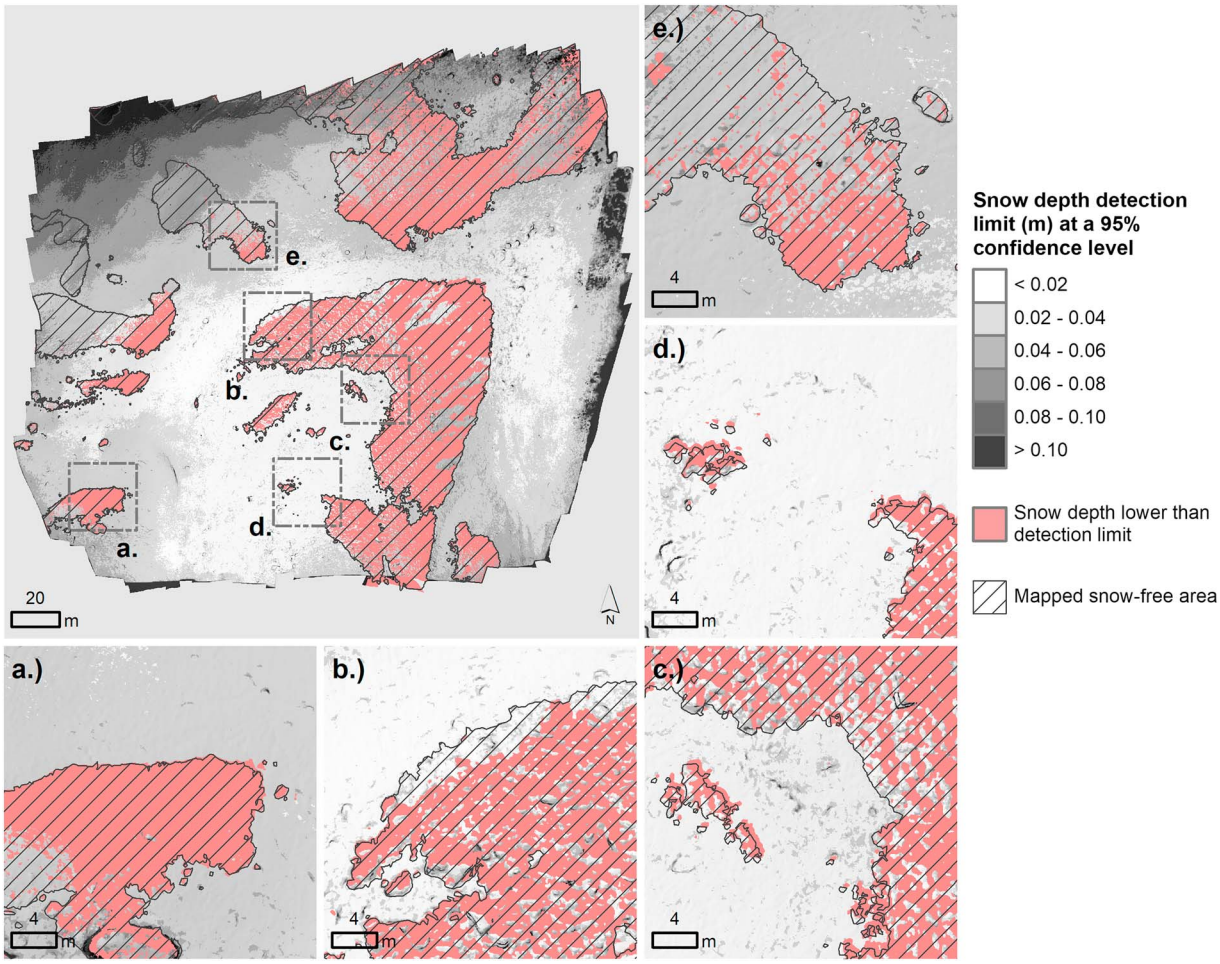

Figure 3. Areas where the structure-from-motion multiview stereo 3-D reconstruction snow depth level was determined to be significant based a *t* test applied for each grid cell at a 0.05 significance level. The snow-free area was mapped from an orthomosaic of the unmanned aerial vehicle imagery.

In general, the precision of the SFM DEMs is related to flying height, distance to GCP, and image overlap (Goetz et al., 2018; James, Robson, Smith, et al., 2017), as well as field site conditions (Bühler, Adams, Bösch, et al., 2016; Nolan et al., 2015). That is, errors in the computed snow depths can also vary temporally due to different snow-cover conditions (Adams et al., 2018; Bühler, Adams, Bösch, et al., 2016; Fernandes et al., 2018; Harder et al., 2016). The precision for most of the study area was less than 4 cm (at 1σ). This precision estimate is based on a flying height of approximately 60 m above ground level. Adams et al. (2018) observed precisions ranging from 4 cm for stable terrain to 33 cm for their entire alpine study area. This weaker precision that they reported is likely due to their higher-flying height of 400 m above ground level. The precision of SFM DEMs can increase with higher flying heights (Goetz et al., 2018). Additionally, like Hendrickx et al. (2019), we observed weaker precision in areas of high surface roughness (i.e., the rocky debris terrain). These areas also corresponded to the highest point densities in the DEMs. In general, higher errors in SFM DEMs can occur in areas of high point densities where image surface textures are more complex (Cook, 2017).

In addition to using the detection limits to determine where significant levels of snow depth were detected, a comparison with a map of snow-free areas helped to identify areas where a bias in the snow depths was present. Bias in SFM snow depths can be caused by coregistration errors (Marti et al., 2016; Nuth & Kääb, 2011; Westoby et al., 2012), changes in the subsnow topography between snow-on and snow-off DEM acquisition dates (Avanzi et al., 2018; Bernard et al., 2017; Gindraux et al., 2017; Nolan et al., 2015), and a systematic "doming" error in the SFM DEMs (James & Robson, 2014; Micheletti et al., 2015). The pattern in the

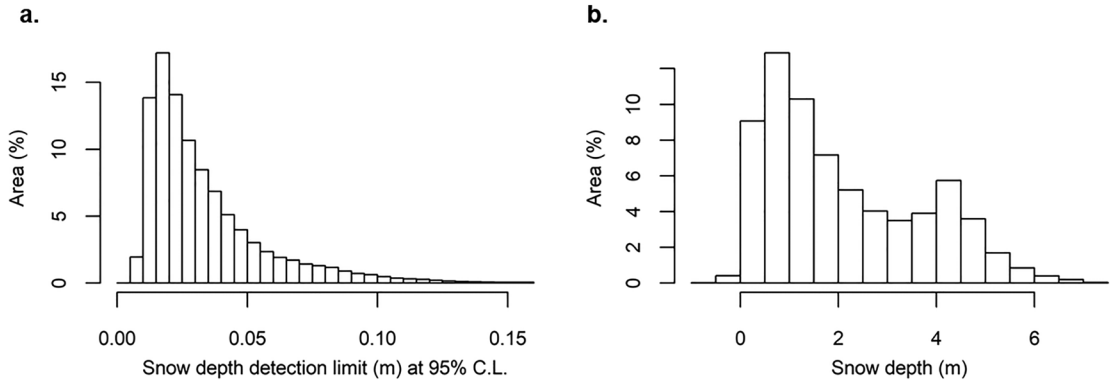

Figure 4. Histograms of the spatially varying snow depth detection limit at a 95% confidence level (a) and structure-from-motion multiview stereo 3-D reconstruction snow depths (b).

GNSS-measured errors of the snow-on DEM did show signs of such as doming error (Figure 2a). This error is likely due to the poor image collection geometry caused by the UAV imagery being taken at near-parallel directions and an inaccurate camera model (Micheletti et al., 2015). Perhaps, this error was only observed outside the area enclosed by the GCPs because the error is locally improved near GCPs (James & Robson, 2014; Javernick et al., 2014). Visualizing the spatially variation in detection limits also helped to provide evidence for why higher snow depths errors occurred on the rock glacier, for example, by observing changes in the ground topography.

4.2. Limitations of Methods for Mapping SFM Uncertainties

In this study, the spatially varying precision estimates and subsequent detection limits were calculated using repeated UAV surveys to obtain multiple SFM DEM observations. This method estimates the actual variability in surface elevation per grid cell from one UAV survey to another, which is its main strength. It includes factors that influence precision such as weather, changes in lighting conditions, flight characteristics, and SFM processing. However, depending on the size of the surveying area, repeat UAV surveys may be difficult to perform due to time constraints, which can be particularly challenging in alpine environments due to quickly changing optimal weather conditions (Bühler, Adams, Stoffel, et al., 2016). Therefore, for SFM snow depth mapping of larger areas with UAVs, it may be more practical to use methods that estimate precision from a single UAV survey such as the Multiscale Model to Model Cloud Comparison method that utilizes local variation in dense point locations to determine precision (Lague et al., 2013) or the method illustrated by James, Robson, Smith, et al. (2017) that estimates sparse point cloud precision from the variation in bundle adjustment parameters and Monte Carlo simulations. However, these methods also have some limitations.

Since the Multiscale Model to Model Cloud Comparison method is based solely on a single realization of the SFM reconstructed surface, it may not account for the variation in elevations that can occur from random subprocedures in the SFM processing (e.g., Dickscheid et al., 2008): Hendrickx et al. (2019) observed that elevations can vary up 10 cm for steep slope areas and up to 3 m at edges of a scene due to SFM processing alone. The repeated UAV surveys and the Monte Carlo simulation methods include this variation since they utilize multiple SFM reconstruction realizations. The method illustrated by James, Robson, Smith, et al. (2017) has the limitation that precision is only determined for the sparse point cloud (i.e., tie points), meaning that a well-distributed sparse point cloud is required to obtain good spatial coverage of precision estimates. Additionally, the sparse point cloud precisions must be interpolated to the corresponding dense point cloud or DEM for continuous spatial coverage. Performing this interpolation can be difficult for snow-covered terrain due to issues in obtaining well-distributed tie points when the snow cover image texture appears smooth and homogeneous (Bühler, Adams, Bösch, et al., 2016; Cimoli et al., 2017).

Given the limitation of these methods, repeated UAV surveys may be the most robust approach to determine the spatial variation in precision with continuous spatial coverage for various snow-covered terrain conditions. Therefore, it is suggested that at least a detailed uncertainty analysis or a pilot test of the UAV and

SFM survey design for a small segment of a study area is performed, for example, using repeated UAV flights. By doing so, a better picture can be drawn of how the particular camera sensor, distribution of ground control, environmental conditions, UAV survey design, and SFM-MVS software will affect DEM uncertainty to assure the quality of the SFM snow depths for a given application (Benassi et al., 2017; Goetz et al., 2018; Hendrickx et al., 2019; James, Robson, d'Oleire-Oltmanns, et al., 2017; Smith et al., 2015).

4.3. Reducing SFM Snow Depth Uncertainties

When designing a survey for snow depth monitoring with SFM photogrammetry, just as with lidar (Csanyi & Toth, 2007) and digital photogrammetry (Barrand et al., 2009), it is important to ensure that in each survey, the spatial distribution of GCPs encloses the entire area of interest. Otherwise, data may be lost due to low-precision observations or more likely due to a strong bias in one of the DEMs that can lead to an overestimation or underestimation of snow depth, as was observed in this study.

Depending on the desired accuracy and precision of the snow depth estimates, it is also important to ensure that the GCPs are evenly spaced out to control the amount of measurement uncertainty. In this study, a high GCP density network was used to ensure that we would obtain a high-quality snow-on and snow-off DEMs for our local case study over the rock glacier. For larger-scale applications, such a high density (~300 GCPs per km^2) is not practical and may not be necessary for obtaining quality SFM snow depths. Gindraux et al. (2017) determined for SFM reconstruction with an average UAV flying height of 115 m above ground level that the accuracy of the SFM DEMs did not significantly improve for a ground control network with more than 17 GCPs per km^2. Similar to Tonkin and Midgley (2016), they also found that substantial decrease in DEM accuracy occurred at distances greater than 100 m from GCP. Denser networks of GCPs are generally required when the image network and subsequent SFM camera model are poor (James, Robson, Smith, et al., 2017; Javernick et al., 2014). Adding oblique imagery instead of using only nadir viewing angles or including more images (e.g., higher image overlap) can improve the quality of SFM reconstruction without having to rely solely on GCPs for mitigating SFM reconstruction errors (James & Robson, 2014; James, Robson, d'Oleire-Oltmanns, et al., 2017). Additionally, the density of the GCP network can be further reduced with the use of RTK or post-processing kinematic solutions for correction of the UAVs onboard GNSS for higher-quality camera location estimates (Fernandes et al., 2018; James, Robson, d'Oleire-Oltmanns, et al., 2017). Therefore, by surveying with a strong image network, using high-quality geotagging and ground control (e.g., RTK/PKK GNSS measurements), large-scale SFM snow depth mapping is likely more feasible.

Accurate georeferencing of the SFM DEMs is also important for reducing the uncertainties and improving the accuracy of computed snow depths. Due to the constantly changing topography of a snow-covered surface, especially just after recent snowfall, there may be occasions when there are no exposed snow-free areas that could allow for coregistration of the snow-on and snow-off DEMs to reduce any potential registration biases. Also, the constantly changing snow-covered topography makes it difficult to have GCPs located in the same place (Bernard et al., 2017). In such scenarios, only the positional accuracy of the GCPs measured by a GNSS survey are relied on for the registration of the DEMs. In this study, a local reference GNSS station was used to ensure high-quality positional estimates of the GCPs. Using this approach, it was demonstrated that an overall snow depth accuracy of 15 cm and a precision of the snow depth measurements of approximately less than 5 cm can be achieved when the coregistration relies solely on the georefencing of snow-on and snow-off DEMs. Multiple SFM DEMs can closely match the same reference datum given the quality of the reconstructed surface is good and the precision of GNSS-surveyed control strong (James, Robson, Smith, et al., 2017). Therefore, the accuracy of the SFM snow depths computed without additionally coregistration may be reduced by improving the positional estimates (i.e., GNSS precision) of the GCP locations.

5. Conclusions

This study presented a method for calculating a spatially varying estimate of snow depth precision and detection limits using repeated UAV surveys. The map of snow depth precision is important for communicating the distribution of uncertainties in the snow depths. Through applying the spatially varying detection limits, it was found that it is possible to observe snow depths generally as low as 2 cm with 95% confidence from UAV imagery and SFM photogrammetry. Performing such an uncertainty analysis can be used to provide

strong support for the quality of the SFM snow depths. We also observed higher SFM snow depth errors on the rock glacier compared to the adjacent stable terrain. Visualizing the spatially varying detection limits was useful for highlighting areas where possible snow depth biases were present, such as due to changing ground topography between DEM acquisition dates. Identifying areas that may have a strong bias in the calculated snow depths can be used to delineate the boundaries of the study area where the data quality is acceptable. It is also recommended to ensure that the area covered by the GCPs is the same for the snow-on and snow-off DEMs to avoid losing data due to poor SFM performance in areas more distant from ground control locations. Overall, the methods used in this study can be applied to help identify limitations and ways to improve SFM snow depth mapping for different field sites and snow cover conditions.

Acknowledgments

Thanks to the Parc national des Ecrins and the Joseph Fourier Alpine Research Station (SAFJ) for their support and everyone who assisted in the field. Also, thanks to the anonymous reviewers for their constructive comments that helped improve this paper. The Natural Sciences and Engineering Research Council (NSERC) of Canada through an Alexander Graham Bell Graduate Scholarship awarded to J. Goetz and funding from the Carl Zeiss Foundation awarded to A. Brenning have supported this research. The data used in this study (i.e., DEMs, UAV imagery, ground control locations, snow-probed depths, and GNSS survey data) are available in the Mendeley research data repository: Goetz, J., A. Brenning., M. Marcer, and X. Bodin (2019), UAV imagery and in-situ measurements for structure-from-motion snow depth mapping over the Laurichard rock glacier, France - surveyed in 2017, *Mendeley Data*, *v1* (https://doi.org/10.17632/9rhscd27y4.1).

References

Adams, M. S., Bühler, Y., & Fromm, R. (2018). Multitemporal accuracy and precision assessment of unmanned aerial system photogrammetry for slope-scale snow depth maps in alpine terrain. *Pure and Applied Geophysics*, *175*(9), 3303–3324. https://doi.org/10.1007/s00024-017-1748-y

Apaloo, J., Brenning, A., & Bodin, X. (2012). Interactions between seasonal snow cover, ground surface temperature and topography (Andes of Santiago, Chile, 33.5°S). *Permafrost and Periglacial Processes*, *23*(4), 277–291. https://doi.org/10.1002/ppp.1753

Avanzi, F., Bianchi, A., Cina, A., de Michele, C., Maschio, P., Pagliari, D., et al. (2018). Centimetric accuracy in snow depth using unmanned aerial system photogrammetry and a multistation. *Remote Sensing*, *10*(5), 765. https://doi.org/10.3390/rs10050765

Barnett, T. P., Adam, J. C., & Lettenmaier, D. P. (2005). Potential impacts of a warming climate on water availability in snow-dominated regions. *Nature*, *438*(7066), 303–309. https://doi.org/10.1038/nature04141

Barrand, N. E., Murray, T., James, T. D., Barr, S. L., & Mills, J. P. (2009). Optimizing photogrammetric DEMs for glacier volume change assessment using laser-scanning derived ground-control points. *Journal of Glaciology*, *55*(189), 106–116.

Benassi, F., Dall'Asta, E., Diotri, F., Forlani, G., Di Morra Cella, U., Roncella, R., & Santise, M. (2017). Testing accuracy and repeatability of UAV blocks oriented with GNSS-supported aerial triangulation. *Remote Sensing*, *9*(2), 172. https://doi.org/10.3390/rs9020172

Bernard, É., Friedt, J. M., Tolle, F., Griselin, M., Marlin, C., & Prokop, A. (2017). Investigating snowpack volumes and icing dynamics in the moraine of an Arctic catchment using UAV photogrammetry. *The Photogrammetric Record*, *32*(160), 497–512. https://doi.org/10.1111/phor.12217

Bodin, X., Thibert, E., Fabre, D., Ribolini, A., Schoeneich, P., Francou, B., et al. (2009). Two decades of responses (1986-2006) to climate by the Laurichard rock glacier, French Alps. *Permafrost and Periglacial Processes*, *20*(4), 331–344. https://doi.org/10.1002/ppp.665

Borradaile, G. (2002). *Statistics of earth science data: Their distribution in time, space and orientation*. New York, London: Springer.

Brasington, J., Langham, J., & Rumsby, B. (2003). Methodological sensitivity of morphometric estimates of coarse fluvial sediment transport. *Geomorphology*, *53*(3-4), 299–316. https://doi.org/10.1016/S0169-555X(02)00320-3

Brasington, J., Rumsby, B. T., & McVey, R. A. (2000). Monitoring and modelling morphological change in a braided gravel-bed river using high resolution GPS-based survey. *Earth Surface Processes and Landforms*, *25*(9), 973–990. https://doi.org/10.1002/1096-9837(200008)25:9<973::AID-ESP111>3.0.CO;2-Y

Bühler, Y., Adams, M. S., Bösch, R., & Stoffel, A. (2016). Mapping snow depth in alpine terrain with unmanned aerial systems (UAS): Potential and limitations. *The Cryosphere*, *10*(3), 1075–1088. https://doi.org/10.5194/tc-10-1075-2016

Bühler, Y., Adams, M. S., Stoffel, A., & Boesch, R. (2016). Photogrammetric reconstruction of homogenous snow surfaces in alpine terrain applying near-infrared UAS imagery. *International Journal of Remote Sensing*, *38*(8-10), 3135–3158. https://doi.org/10.1080/01431161.2016.1275060

Bühler, Y., Christen, M., Kowalski, J., & Bartelt, P. (2011). Sensitivity of snow avalanche simulations to digital elevation model quality and resolution. *Annals of Glaciology*, *52*(58), 72–80. https://doi.org/10.3189/172756411797252121

Cimoli, E., Marcer, M., Vandecrux, B., Bøggild, C. E., Williams, G., & Simonsen, S. B. (2017). Application of low-cost UASs and digital photogrammetry for high-resolution snow depth mapping in the Arctic. *Remote Sensing*, *9*(11), 1144. https://doi.org/10.3390/rs9111144

Cook, K. L. (2017). An evaluation of the effectiveness of low-cost UAVs and structure from motion for geomorphic change detection. *Geomorphology*, *278*, 195–208. https://doi.org/10.1016/j.geomorph.2016.11.009

Csanyi, N., & Toth, C. K. (2007). Improvement of lidar data accuracy using lidar-specific ground targets. *Photogrammetric Engineering and Remote Sensing*, *73*(4), 385–396. https://doi.org/10.14358/PERS.73.4.385

de Michele, C., Avanzi, F., Passoni, D., Barzaghi, R., Pinto, L., Dosso, P., et al. (2016). Using a fixed-wing UAS to map snow depth distribution: An evaluation at peak accumulation. *The Cryosphere*, *10*(2), 511–522. https://doi.org/10.5194/tc-10-511-2016

Delaloye, R., Lambiel, C., & Gärtner-Roer, I. (2010). Overview of rock glacier kinematics research in the Swiss Alps. *Geography Helvetiae*, *65*(2), 135–145. https://doi.org/10.5194/gh-65-135-2010

Dickscheid, T., Labe, T., & Förstner, W. (2008). Benchmarking automatic bundle adjustment results. In J. Chen, et al. (Eds.), *21st Congress of the International Society for Photogrammetry and Remote Sensing (ISPRS)*, (pp. 7–12). x: x.

Fernandes, R., Prevost, C., Canisius, F., Leblanc, S. G., Maloley, M., Oakes, S., et al. (2018). Monitoring snow depth change across a range of landscapes with ephemeral snowpacks using structure from motion applied to lightweight unmanned aerial vehicle videos. *The Cryosphere*, *12*(11), 3535–3550. https://doi.org/10.5194/tc-12-3535-2018

Fonstad, M. A., Dietrich, J. T., Courville, B. C., Jensen, J. L., & Carbonneau, P. E. (2013). Topographic structure from motion: A new development in photogrammetric measurement. *Earth Surface Processes and Landforms*, *38*(4), 421–430. https://doi.org/10.1002/esp.3366

Gindraux, S., Boesch, R., & Farinotti, D. (2017). Accuracy assessment of digital surface models from unmanned aerial vehicles' imagery on glaciers. *Remote Sensing*, *9*(2), 186. https://doi.org/10.3390/rs9020186

Goetz, J., Brenning, A., Marcer, M., & Bodin, X. (2018). Modeling the precision of structure-from-motion multi-view stereo digital elevation models from repeated close-range aerial surveys. *Remote Sensing of Environment*, *210*, 208–216. https://doi.org/10.1016/j.rse.2018.03.013

Goetz, J., Fieguth, P., Kasiri, K., Bodin, X., Marcer, M., & Brenning, A. (2019). Accounting for permafrost creep in high-resolution snow depth mapping by modelling sub-snow ground deformation. *Remote Sensing of Environment*, *231*, 111275. https://doi.org/10.1016/j.rse.2019.111275

Haberkorn, A., Phillips, M., Kenner, R., Rhyner, H., Bavay, M., Galos, S. P., & Hoelzle, M. (2016). Thermal regime of rock and its relation to snow cover in steep alpine rock walls: Gemsstock, central swiss alps, *Geografiska Annaler: Series A. Physical Geography*, *97*(3), 579–597. https://doi.org/10.1111/geoa.12101

Harder, P., Schirmer, M., Pomeroy, J., & Helgason, W. (2016). Accuracy of snow depth estimation in mountain and prairie environments by an unmanned aerial vehicle. *The Cryosphere*, *10*(6), 2559–2571. https://doi.org/10.5194/tc-10-2559-2016

Hendrickx, H., Vivero, S., de Cock, L., de Wit, B., de Maeyer, P., Lambiel, C., et al. (2019). The reproducibility of SfM algorithms to produce detailed digital surface models: The example of PhotoScan applied to a high-alpine rock glacier. *Remote Sensing Letters*, *10*(1), 11–20. https://doi.org/10.1080/2150704X.2018.1519641

Hijmans, R. J. (2016), raster: Geographic data analysis and modeling. R package version 2.5-8., https://CRAN.R-project.org/package=raster.

Ikeda, A., Matsuoka, N., & Kääb, A. (2008). Fast deformation of perennially frozen debris in a warm rock glacier in the Swiss Alps: An effect of liquid water. *Journal of Geophysical Research*, *113*(F1), 212. https://doi.org/10.1029/2007JF000859

Immerzeel, W. W., Kraaijenbrink, P. D. A., Shea, J. M., Shrestha, A. B., Pellicciotti, F., Bierkens, M. F. P., & de Jong, S. M. (2014). High-resolution monitoring of Himalayan glacier dynamics using unmanned aerial vehicles. *Remote Sensing of Environment*, *150*, 93–103. https://doi.org/10.1016/j.rse.2014.04.025

James, M. R., & Robson, S. (2012). Straightforward reconstruction of 3D surfaces and topography with a camera: Accuracy and geoscience application. *Journal of Geophysical Research*, *117*(F3), F03017. https://doi.org/10.1029/2011JF002289

James, M. R., & Robson, S. (2014). Mitigating systematic error in topographic models derived from UAV and ground-based image networks. *Earth Surface Processes and Landforms*, *39*(10), 1413–1420. https://doi.org/10.1002/esp.3609

James, M. R., Robson, S., d'Oleire-Oltmanns, S., & Niethammer, U. (2017). Optimising UAV topographic surveys processed with structure-from-motion: Ground control quality, quantity and bundle adjustment. *Geomorphology*, *280*, 51–66. https://doi.org/10.1016/j.geomorph.2016.11.021

James, M. R., Robson, S., & Smith, M. W. (2017). 3-D uncertainty-based topographic change detection with structure-from-motion photogrammetry: Precision maps for ground control and directly georeferenced surveys. *Earth Surface Processes and Landforms*, *42*(12), 1769–1788. https://doi.org/10.1002/esp.4125

Javernick, L., Brasington, J., & Caruso, B. (2014). Modeling the topography of shallow braided rivers using structure-from-motion photogrammetry. *Geomorphology*, *213*, 166–182. https://doi.org/10.1016/j.geomorph.2014.01.006

Jonas, T., Rixen, C., Sturm, M., & Stoeckli, V. (2008). How alpine plant growth is linked to snow cover and climate variability. *Journal of Geophysical Research*, *113*(G3), 377. https://doi.org/10.1029/2007JG000680

Lague, D., Brodu, N., & Leroux, J. (2013). Accurate 3D comparison of complex topography with terrestrial laser scanner: Application to the Rangitikei canyon (N-Z). *ISPRS Journal of Photogrammetry and Remote Sensing*, *82*, 10–26. https://doi.org/10.1016/j.isprsjprs.2013.04.009

Lane, S. N., Westaway, R. M., & Murray Hicks, D. (2003). Estimation of erosion and deposition volumes in a large, gravel-bed, braided river using synoptic remote sensing. *Earth Surface Processes and Landforms*, *28*(3), 249–271. https://doi.org/10.1002/esp.483

Lemke, P., Ren, J., Alley, R. B., Allison, I., Carrasco, J., Flato, G., et al. (2007). Observations: Changes in snow, ice and frozen ground. In M. L. Parry (Ed.), *Climate change 2007: The physical science basis; summary for policymakers, technical summary and frequently asked questions. Part of the Working Group I contribution to the Fourth Assessment Report of the Intergovernmental Panel on Climate Change* (Chap. 4, pp. 337–383). New York: Cambridge University Press.

Luetschg, M., & Haeberli, W. (2007). Permafrost evolution in the Swiss Alps in a changing climate and the role of the snow cover. *Norsk Geografisk Tidsskrift - Norwegian Journal of Geography*, *59*(2), 78–83. https://doi.org/10.1080/00291950510020583

Marti, R., Gascoin, S., Berthier, E., de Pinel, M., Houet, T., & Laffly, D. (2016). Mapping snow depth in open alpine terrain from stereo satellite imagery. *The Cryosphere*, *10*(4), 1361–1380. https://doi.org/10.5194/tc-10-1361-2016

Matsuura, S., Asano, S., Okamoto, T., & Takeuchi, Y. (2003). Characteristics of the displacement of a landslide with shallow sliding surface in a heavy snow district of Japan. *Engineering Geology*, *69*(1-2), 15–35. https://doi.org/10.1016/S0013-7952(02)00245-4

Micheletti, N., Chandler, J. H., & Lane, S. N. (2015). Structure from motion (SFM) photogrammetry. In L. E. Clark, & J. M. Nield (Eds.), *Geomorphological techniques* (Chap. 2, section 2.2, pp. 1–12). London: British Society for Geomorphology.

Middelkoop, H., Daamen, K., Gellens, D., Grabs, W., Kwadijk, J. C. J., Lang, H., et al. (2001). Impact of climate change on hydrological regimes and water resources management in the Rhine Basin. *Climatic Change*, *49*(1/2), 105–128. https://doi.org/10.1023/A:1010784727448

Nolan, M., Larsen, C., & Sturm, M. (2015). Mapping snow depth from manned aircraft on landscape scales at centimeter resolution using structure-from-motion photogrammetry. *The Cryosphere*, *9*(4), 1445–1463. https://doi.org/10.5194/tc-9-1445-2015

Nuth, C., & Kääb, A. (2011). Co-registration and bias corrections of satellite elevation data sets for quantifying glacier thickness change. *The Cryosphere*, *5*(1), 271–290. https://doi.org/10.5194/tc-5-271-2011

Okamoto, T., Matsuura, S., Larsen, J. O., Asano, S., & Abe, K. (2018). The response of pore water pressure to snow accumulation on a low-permeability clay landslide. *Engineering Geology*, *242*, 130–141. https://doi.org/10.1016/j.enggeo.2018.06.002

Passalacqua, P., Belmont, P., Staley, D. M., Simley, J. D., Arrowsmith, J. R., Bode, C. A., et al. (2015). Analyzing high resolution topography for advancing the understanding of mass and energy transfer through landscapes: A review. *Earth-Science Reviews*, *148*, 174–193. https://doi.org/10.1016/j.earscirev.2015.05.012

Rossini, M., Di Mauro, B., Garzonio, R., Baccolo, G., Cavallini, G., Mattavelli, M., et al. (2018). Rapid melting dynamics of an alpine glacier with repeated UAV photogrammetry. *Geomorphology*, *304*, 159–172. https://doi.org/10.1016/j.geomorph.2017.12.039

Smith, M. W., Carrivick, J. L., & Quincey, D. J. (2015). Structure from motion photogrammetry in physical geography. *Progress in Physical Geography*, *40*(2), 247–275. https://doi.org/10.1177/0309133315615805

Snavely, N., Seitz, S. M., & Szeliski, R. (2006). Photo tourism: Exploring photo collections in 3D. *ACM Transactions on Graphics*, *25*(3), 835. https://doi.org/10.1145/1141911.1141964

Tinkham, W. T., Smith, A. M. S., Marshall, H.-P., Link, T. E., Falkowski, M. J., & Winstral, A. H. (2014). Quantifying spatial distribution of snow depth errors from LiDAR using Random Forest. *Remote Sensing of Environment*, *141*, 105–115. https://doi.org/10.1016/j.rse.2013.10.021

Tonkin, T., & Midgley, N. (2016). Ground-control networks for image based surface reconstruction: An investigation of optimum survey designs using UAV derived imagery and structure-from-motion photogrammetry. *Remote Sensing*, *8*(9), 786. https://doi.org/10.3390/rs8090786

Tonkin, T. N., Midgley, N. G., Graham, D. J., & Labadz, J. C. (2014). The potential of small unmanned aircraft systems and structure-from-motion for topographic surveys: A test of emerging integrated approaches at Cwm Idwal, North Wales. *Geomorphology*, *226*, 35–43. https://doi.org/10.1016/j.geomorph.2014.07.021

Vander Jagt, B., Lucieer, A., Wallace, L., Turner, D., & Durand, M. (2015). Snow depth retrieval with UAS using photogrammetric techniques. *Geosciences*, *5*(3), 264–285. https://doi.org/10.3390/geosciences5030264

Wechsler, S. P., & Kroll, C. N. (2006). Quantifying DEM uncertainty and its effect on topographic parameters. *Photogrammetric Engineering & Remote Sensing*, *72*(9), 1081–1090. https://doi.org/10.14358/PERS.72.9.1081

Westoby, M. J., Brasington, J., Glasser, N. F., Hambrey, M. J., & Reynolds, J. M. (2012). 'Structure-from-motion' photogrammetry: A low-cost, effective tool for geoscience applications. *Geomorphology*, *179*, 300–314. https://doi.org/10.1016/j.geomorph.2012.08.021

Wheaton, J. M., Brasington, J., Darby, S. E., & Sear, D. A. (2010). Accounting for uncertainty in DEMs from repeat topographic surveys: Improved sediment budgets. *Earth Surface Processes and Landforms*, *35*, n/a–156. https://doi.org/10.1002/esp.1886